

A New Hybrid Wavelet Neural Network and Interactive Honey Bee Matting Optimization Based on Islanding Detection

Nasser Yousefi

Young Researchers and Elite club, Ardabil Branch, Islamic Azad University, Ardabil, Iran
email: nasseryousefi2472@gmail.com

Abstract

In this paper a passive Neuro-wavelet on the basis of islanding detection procedure for grid-connected inverter-based distributed generation has been developed. Moreover, the weight parameters of neural network are optimized by Interactive Honey Bee Matting optimization (IHBMO) to increase the efficiency of the capability of suggested procedure in tendered problem. Islanding is the situation where the distribution system including both distributed generator and loads is disconnected from the major grid as a consequence of lots of reasons such as electrical faults and their subsequent switching incidents, equipment failure, or pre-planned switching events like maintenance. The suggested method uses and combines wavelet analysis and artificial neural network together to detect islanding. It can be used in removing discriminative characteristics from the acquired voltage signals. In passive schemes have a large Non Detection Zone (NDZ), concern has been raised on active method because of its lowering power quality impact. The main focus of the proposed scheme is to decrease the NDZ to as close as possible and to retain the output power quality fixed. The simulations results, performed by MATLAB/Simulink, demonstrate that the mentioned procedure has a small non-detection zone. What is more, this method is capable of detecting islanding precisely within the least possible amount of standard time.

Keywords: IHBMO, islanding detection, neuro-wavelet, non-detection zone, distributed generation

1. Introduction

The traditional distributed generation systems are wind power generation, photovoltaic power generation, fuel cell power generation, and micro-turbine power generation. A Distributed Generator (DG) is usually related to each other with the existing utility grid at one point so that they are dividing the local load. Islanding detection is an important issue when a DG works in connection with the power grid [1]-[3].

Classical view of power system is characterized by a unidirectional power flow from centralized generation to consumers. Power system restructuring gave more emphasis to a modern view by introducing DG into distribution systems, bringing about a bi-directional power flow. In fact, the issue of implanting distributed generation into the distribution system was suggested supposing DGs will always be operating in a grid-connected mode. Anyway, few years later, it has been discerned that several operational issues are associated with distributed generation when operating in an island mode where [4].

Power quality in reverse consists of frequency deviation, voltage fluctuation, harmonics and reliability of the power system. Moreover, one of the specialized notions developed by DG interconnection is accidental islanding [5]-[6]. Islanding condition causes abnormal operation in the power system and negative effects on protection, operation, and handling of distribution systems. Therefore, it is immediately to effectively detect the islanding conditions and promptly disconnect DG from the network.

Within this condition, a supposed island is developed, resulting in unexpected results that may consist of an increased intricacy of orderly reconstruction (out of phase switching of reclosers leading to damage of the DG, nearby loads, and utility equipment), a reduced stability of system voltage and worst of all, an increased risk to related maintenance personnel. In other words, under the scenario of islanding, line crewmembers may err in evaluation the load-side of the line as passive where distributed generations are in fact feeding power to loads; therefore endangering the life of operators and in the intervening time providing explanations on the importance of a credible alert behavior to such events. Therefore, during the interruptions of

utility power, the related DG must detect the loss of utility power and disconnect itself from the power grid quickly [7].

There are many suggested procedures for detection of an island [8]-[17]. The NDZ can be described and elaborated on as the domain (in terms of the power difference between the DG inverter and the load or load parameters) in which an islanding detection scheme under examination fails to detect this situation [10]. The second characteristic is related to the type of loads (potential loads inside island), which can be modeled as a parallel RLC circuit. This circuit is mainly utilized because it causes more difficulties for islanding detection techniques than others. [11]. Most islanding detection procedures suffer from large NDZs [18]-[19] and/or have a run-on time between half a second to two seconds [20], and therefore cannot be utilized for uninterruptible independent operation of an island. These procedures can be mainly categorized into far and local procedures. Local procedure can be divided into active and passive ones. It is clear that these procedures may have better reliability than local procedures; so they are expensive to performance and hence uneconomical. These schemes consist of power line signaling and transfer trip [21]-[22]. Local procedures count on the information and data at the DG site. Passive procedures depend on measuring specific system parameters and do not interfere with the DG operation. One of the simplest passive methods used in islanding detection is over/under voltage and frequency. In any event, if the load and the generation on the island are precisely compatible, the change in voltage and frequency may be very trivial and within the thresholds, therefore causing an undetected islanding situation. The other inactive procedures have been suggested on the basis of controlling rate of change of frequency (ROCOF), phase angle displacement, rate of change of generator power output, impedance monitoring, the THD producer and the wavelet transform function [23]. These offer superior sensitivity as their settings allow detection to take place within statutory limits, but their settings must be attentively chosen to prevent mal-operation during network faults.

In this paper, a passive Neuro-wavelet based islanding detection procedure decreasing the NDZ to as close as possible and to hold the output power quality fixed has been extended. The suggested strategy utilizes and combines wavelet analysis and artificial neural network to detect islanding. The suggested strategy is based on the transient voltage signals generated during the islanding event. Discrete wavelet transform is powerful of decomposing the signals into different frequency bands. It can be used in finding discriminative characteristics from the achieved voltage signals. Then, the characteristics are fed to a trained artificial neural network model which is well trained puissant of differentiating among islanding event and any other transient events such as switching or temporary fault. The trained compositor was tested with the use of novel voltage waveforms. The obtained results demonstrate that this approach can detect islanding events with high degree of accuracy.

The problem model is suited for usages of Interactive Honey Bee Matting optimization (IHBMO) to find the optimal weight parameters of neural network. The HBMO is a partly recently developed procedure that has been empirically demonstrated to perform well on many of these optimization problems [24]-[27]. This optimization method has been widely utilized to solve different problems particularly the locating problems in power system. This work shows the combining procedure by regarding the universal gravitation between queen and drone bees for the standard HBMO algorithm to recover condition called the IHBMO.

This paper is organized as follows. Section II presents the problem statement. The impact of the interface control on the NDZ of over/under voltage and frequency protection (OVP/UVP) and OFP/UFP is discussed in Section III. Section IV presents the suggested procedure structure. In section V the mentioned IHBMO is demonstrated. Section VI provides the simulation results to verify the effectiveness of the suggested procedure and the conclusion will be presented in the last section of this paper

2. Problem Statement

The islanding detection schemes suggested in literature can be categorized into two classes: far and local as demonstrated in Figure 1. Islanding detection schemes are effectively evaluated based on the NDZ. The NDZ corresponds to the range of active and reactive load-generation mismatches within the island in which the islanding detection method fails to identify the islanding state.

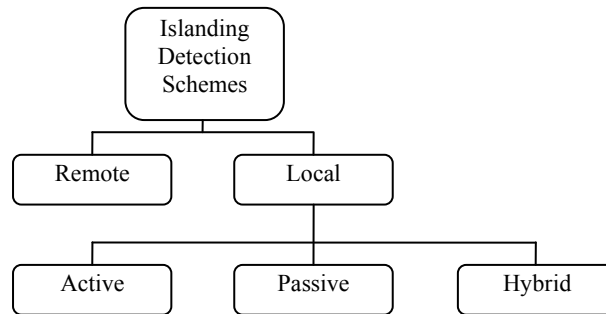


Figure 1. Classification of islanding detection schemes

This section explains a state-space mathematical model for the islanded system. It is supposed that the DG unit and the local load are stable three-phase subsystems within the island. The state space equations of the potential island in the standard state space form are.

$$\begin{aligned}
 \dot{X}(t) &= AX(t) + Bu(t) \\
 y(t) &= CX(t) \\
 u(t) &= v_{id}
 \end{aligned} \tag{1}$$

Where

$$A = \begin{bmatrix} -\frac{R_t}{L_t} & \omega_0 & 0 & -\frac{1}{L_t} \\ \omega_0 & -\frac{R_1}{L} & -2\omega_0 & \left(\frac{R_1 C \omega_0}{L} - \frac{\omega_0}{R}\right) \\ 0 & \omega_0 & -\frac{R_1}{L} & \left(\frac{1}{L} - \omega_0^2 C\right) \\ \frac{1}{C} & 0 & -\frac{1}{C} & -\frac{1}{RC} \end{bmatrix}$$

$$B^T = \begin{bmatrix} \frac{1}{L_t} & 0 & 0 & 0 \end{bmatrix}$$

$$C = [0 \quad 0 \quad 0 \quad 1]$$

$$D = [0]$$

$$X^T = [i_{td} \quad i_{tq} \quad i_{Ld} \quad v_d]$$
(2)

Figure 2 demonstrates the step response of system in the islanding mode. There sponse time constant of the island system is chosen as the analyzing time of ANFIS system output.

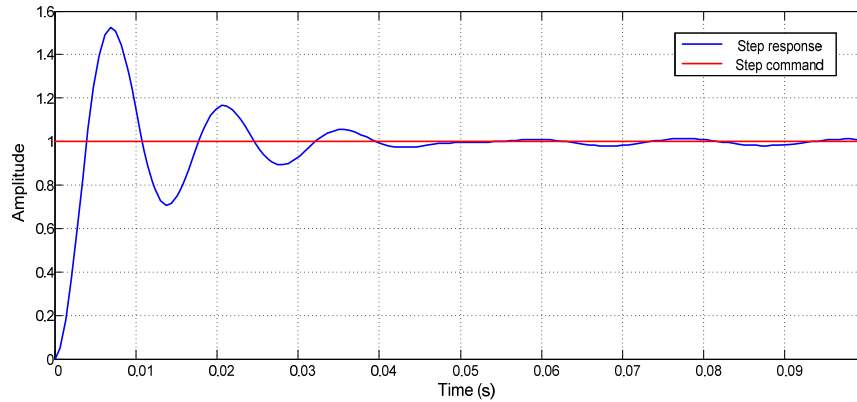


Figure 2. The step response of system in the islanding mode

The system under the research includes one 80kW inverter based DG connected to an RLC load having a quality factor of 1.8 and a grid. The system, controller, and load parameters are given in [6]. The performance of the DG under normal and islanded operating conditions was studied and simulated on MATLAB/SIMULINK. The inverter performs two major functions:

- A) Controlling the active power output of the DG and, in some times, injecting a suitable amount of reactive power to decrease a power quality problem.
- B) On the basis of the IEEE Standard 1547, the DG should be provided with an anti-islanding detection algorithm, which could be performed utilizing the inverter interface control.

The DG interface control is designed to supply constant current output as demonstrated in [6]. For this interface control, both I_d and I_q components of the DG output current are controlled to be equal to a predetermined value (I_{dref} and I_{qref}). The DG was operated at unity power factor by determining I_{qref} to zero. Specifically, parallel RLC loads with a high Q factor often present problems for island detection. The quality factor Q is explained by

$$Q_f = R \sqrt{\frac{C}{L}} \tag{3}$$

And is the ratio of the quantity of energy stored in the load's reactive components to the quantity of energy dissipated in the load's resistance. (For example, for $Q = 2$, there is twice as much energy stored in the L and C of the load as is being dissipated in R) Loads that are near resonance at ω_0 and have a high Q-factor are the ones that cause difficulty in islanding detection. Unhappily, the level of real or reactive power mismatch is not exceptionally determined by load parameters. Particularly, the reactive power consumption of the load is given by

$$Q_{Load} = V_{rms}^2 [(\omega L)^{-1} - (\omega C)] = \Delta Q \tag{4}$$

Equation (3) clearly demonstrating that there are infinitely many combinations of L and C that will produce the same ΔQ .

3. Non Detection Zone (NDZ)

A procedure causing a smaller NDZ will be able to detect the islanding more reliably. It can either be demonstrated in terms of power mismatch or in terms of the R, L, and C of the load. In [6],[28], an approaching representation of the NDZ for OVP/UVP was extracted. An

exact and precise representation of the NDZ is presented in this part of paper. The paper studies the NDZ of an OVP/UVP and OFP/UVP islanding scheme when implemented for constant current controlled inverters. In order to determine the quantity of mismatch for which the OVP/UVP and OFP/UFP will fail to detect islanding, the quantity of active power mismatch in terms of load resistance can be demonstrated as follows:

$$\Delta P = 3V \times I - 3(V + \Delta V) \times I = -3V \times \Delta V \times I \quad (5)$$

Which V and I represent the rated current and voltage, respectively. In distribution network, voltage values between 0.88 pu and 1.1 pu are in acceptable range for voltage relays. These voltage levels are equivalent to $\Delta V = -0.12$ and $\Delta V = 0.1$, respectively. The estimated inequality quantity for our test network (the inverter rated output power is 80kW), are 9.6 kW and -8kW, respectively. Frequency and voltage of an RLC load has the active and reactive power as follows:

$$P_L = \frac{V_L^2}{R_L}$$

$$Q_L = V_L^2 \left(\frac{1}{\omega L} - \omega C \right) \quad (6)$$

Where V , ω , P and Q are the load voltage, frequency, active power and reactive power, respectively. In usual operating situations, a common coupling point voltage is caused by the power grid, and distributed generation system has no control overvoltage and until it is connected to the network the voltage is unchanged at nominal value of 1 pu. Once the island is took place, distribution system cannot control the voltage and the amount of active power imbalance determines the voltage deviation from the nominal values. Since the output power of the inverter is in unity power factor, before islanding reactive power of load is supplied just by network and after islanding the quantity of reactive power imbalance is equal to the consumed load before islanding, hence we have:

$$\Delta Q = 3 \frac{V^2}{\omega_n L} (1 - \omega^2 LC) = 3 \frac{V^2}{\omega_n L} \left(1 - \frac{\omega_n^2}{\omega_r^2} \right) \quad (7)$$

Where ω_n and ω_r are system frequency and resonance frequency of load, respectively. Reactive power imbalance results in the resonance frequency, then the frequency alters after the islanding happening equals the difference between network frequency and load resonance frequency.

$$\omega_r = \omega_n \pm \Delta \omega, \omega_r = \frac{1}{\sqrt{LC}} \quad (8)$$

Thus, the reactive power imbalance needed for certain changes in frequency can be achieved by,

$$\Delta Q = 3 \frac{V^2}{\omega_n L} \left(1 - \frac{f_n^2}{(f_n \pm \Delta f)^2} \right) \quad (9)$$

In distribution network of Iran, the acceptable frequency range is between 49.7 and 50.3Hz which are equal to $\Delta f = -0.3$ and $\Delta f = 0.3$ Hz. In this paper test system, as shown in Figure 3 the quantities of reactive power imbalances are 3.05 and -5.16 kVA, respectively.

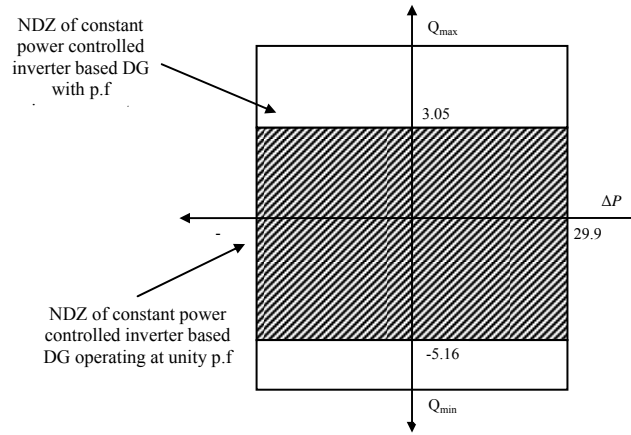


Figure 3. NDZ for the constant current interface controls for distributed generation

4. Interactive Honey Bee Mating optimization

In this part the standard HBMO closely presented. For better illustration see ref [24]. At the beginning of the flight, the queen is initialized with some energy content and returns to her nest when her energy is within some threshold from zero or when her sperm theca is full. In extending the algorithm, the usefulness of workers is limited to brood care, and therefore, each worker may be demonstrated as a heuristic which acts to improve and/or take care of a set of broods. A drone mates with a queen probabilistically using an annealing function as:

$$prob(Q, D) = e^{-\frac{\Delta(f)}{S(t)}} \tag{10}$$

Where Prob (Q, D) is the probability of adding the sperm of drone D to the spermatheca of queen Q (that is, the probability of a successful mating); $\Delta(f)$ is the absolute difference between the fitness of D (i.e., $f(D)$) and the fitness of Q (i.e., $f(Q)$); and $S(t)$ is the speed of the queen at time t . After each transition in space, the queen's speed, $S(t)$, and energy, $E(t)$, decay utilizing the following equations:

$$S(t+1) = \alpha_{HBMO} \times S(t)$$

$$E(t+1) = E(t) - \gamma_{HBMO} \tag{11}$$

Where $\alpha_{HBMO}(t)$ is speed decreasing factor and γ_{HBMO} is the quantity of energy decreasing after each transition ($\alpha, \gamma \in [0, 1]$).

to overcome the drawbacks of classic HBMO, the Interactive Honey Bee Mating Optimization (IHBMO) algorithm is suggested based on the structure of original HBMO algorithm. The gravitational force between two particles (F_{12}) with the mass of the first and second particles (m_1 and m_2), and the distance between them (r_{12}) can be shown as:

$$F_{12} = G \frac{m_1 m_2}{r_{21}^2} \hat{r}_{21} \tag{12}$$

Where, G is gravitational constant. \hat{r}_{21} denotes the unit vector in:

$$\hat{r}_{21} = \frac{r_2 - r_1}{|r_2 - r_1|} \tag{13}$$

In the optimization method with IHBMO algorithm, the mass m_1 is replaced by the symbol, $F(\text{parent}_i)$, which is the fitness value of the queen bee that picked by applying the mating wheel selection. The mass, m_2 , is replaced by the fitness value of the randomly chosen drone bee and is denoted by the parameter, $F(\text{parent}_k)$. The universal gravitation is formed in the vector format. Thus, the quantities of it on different dimensions can be considered separately [27]. Therefore, r_{21} is calculated by taking the difference between the objects only on the concerned dimension currently and the universal gravitation on each dimension is calculated separately. In other words, the intensity of the gravitation on different dimensions is calculated one by one. Therefore, the gravitation on the j th dimensions between parent_i and parent_k can be shown in the below equation. Finally, the below equation can be modified in iteration interval t :

$$F_{ik_j} = G \frac{F(\text{parent}_i) \times F(\text{parent}_k)}{(\text{parent}_{kj} - \text{parent}_{ij})^2} \cdot \frac{\text{parent}_{kj} - \text{parent}_{ij}}{|\text{parent}_{kj} - \text{parent}_{ij}|} \quad (14)$$

$$\text{child}_{ij}(t+1) = \text{parent}_{ij}(t) + F_{ik_j} \cdot [\text{parent}_{ij}(t) - \text{parent}_{kj}(t)]$$

Developing the consideration of the universal gravitation between the drone bees, which is picked by the queen bee, and more than one drone bees is obtainable by adding different $F_{ik}[\text{parent} - \text{parent}_i]$. Therefore, the gravitation F_{ik} plays the role of a weight factor controlling the specific weight of $[\text{parent} - \text{parent}_i]$. The normalization process is taken in order to ensure that $F_{ik} \sim U(0, 1)$. Through the normalization of F_{ik} the gravitational constant (G) can be deleted.

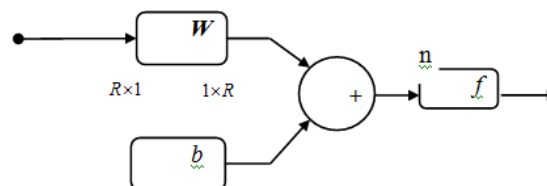
5. Neuro-Wavelet Based Islanding Detection

Recently, wavelet transform has been successfully implemented in solving many power system problems such as fault detection, power quality event localization and load disaggregation. The capability of wavelet in handling non-stationary signals while preserving both time and frequency information makes it a suitable candidate for islanding detection problem.

5.1. Artificial Neural Networks

ANN includes of simple processing units, called neurons, operating in parallel to solve specific problems. Figure 4 demonstrates a simple neuron with input vector P of dimension $R \times 1$. The input P is multiplied by a weight W of dimension $1 \times R$. Therefore, a bias b is added to the product WP . f is a transfer function (called also the activation function) that takes the argument n and produces the net output a .

The idea of ANN is that these parameters (w and p) are adjusted so that the network demonstrates some desired behavior. Therefore, the network can be trained to do a specific job by adjusting the weight or bias parameters [29].



$$a = f(WP + b)$$

Figure 4. Neuron

A number of neurons can be combined together to form a layer of neurons. A one layer of R input elements and S neuron is represented in Figure 5.

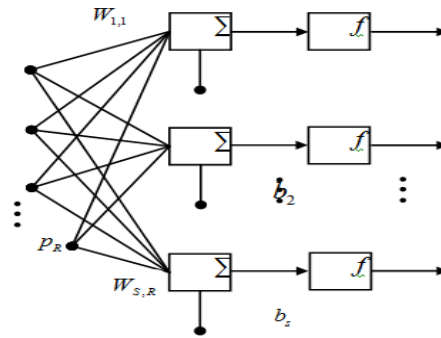


Figure 5. One layer network of R input elements and S neurons

A network can have lots of layers of neurons to form multiple layers of neurons. In Figure 6 three layers of R input elements and S neurons is demonstrated by using the IHBM. The layer that produces the network output is called an output layer. All other layers are called hidden layers. The three layer network is described in Figure 6 has one output layer and two hidden layers.

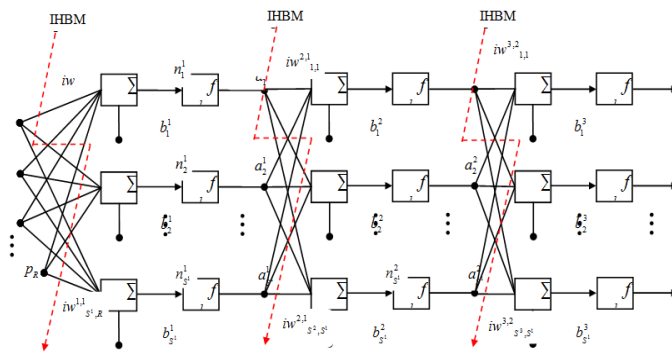


Figure 6. Three layer network of R input elements and S neurons with IHBM

5.2. Training the ANN

A training algorithm is described as a method of updating the weights and biases of a network so the network will be able to perform the specific design task. The training algorithm is divided into two main categories: supervised learning, and unsupervised learning. ANN is categorized under supervised learning. In the training stage, the training data set and the corresponding targets are added into the model. Once the network weights and biases are initialized, the network is ready for training. The weights and biases are then adjusted in order to minimize the Mean Square Error (MSE). This can be achieved using the gradient of the MSE.

Wavelet Transform

WTs can be mainly divided into two classifications: Continuous Wavelet Transform (CWT) and Discrete Wavelet Transform (DWT). The continuous wavelet transform $W(a,b)$ of signal $f(x)$ with respect to a wavelet $\phi(x)$ is given by [30]-[31]:

$$W_{(a,b)} = \frac{1}{\sqrt{a}} \int_{-\infty}^{+\infty} f(x) \phi\left(\frac{x-b}{a}\right) dx \tag{15}$$

Where scale parameter a controls the spread of the wavelet and translation factor b determines its central position. $\phi(x)$ is named mother wavelet. A $W(a,b)$ coefficient, shows how well the original signal $f(x)$ and the scaled/translated mother wavelet match. Thus, the set of all wavelet coefficients $W(a,b)$, associated to a specific signal, is the wavelet showing of the signal with respect to the mother wavelet. It is known as the Discrete Wavelet Transform (DWT):

$$W_{(m,n)} = 2^{-(m/2)} \sum_{t=0}^{T-1} f_{(t)} \phi\left(\frac{t-n \cdot 2^m}{2^m}\right) \quad (16)$$

Where T is the length of the signal $f(t)$. The scaling and translation parameters are functions of the integer variables m and n ($a=2^m$, and $b=n \cdot 2^m$); t is the discrete time index. Daubechies wavelet group is one of the most suitable wavelet families in analyzing power system transients as investigated in [32]. In the present study, the db1 wavelet represented in Figure 7 (with two filter coefficients) has been used as the mother wavelet for analyzing the transients associated with islanding. db1 is a short wavelet and therefore it can efficiently detect transients.

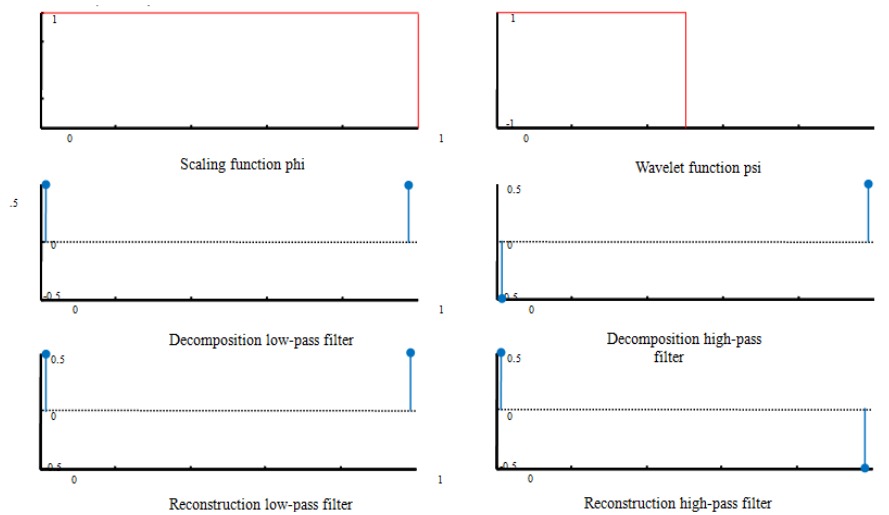


Figure 7. db1 mother wavelet

WT will be carried out on the achieved voltage signals to extract the characteristics. The main target of characteristic extraction is to identify particular signature of the voltage waveforms that can detect islanding and differentiate between islanding and any other transient condition. A transient signal can be completely separated into smoothed signals and detailed signals for L wavelet levels. In wavelets applications, Daubechies wavelet family is one of the most suitable wavelet families in analyzing power wavelet has been utilized as the mother wavelet for extracting the energy content of the detail coefficient of voltage waveforms. db1 is a short wavelet and thus it can efficiently detect transients. The frequency band information of the wavelet analysis is demonstrated in Table 1. The sampling frequency is 10 kHz.

Table 1. Frequency band information for the different levels of wavelet analysis

Wavelet Level	Frequency Band (Hz)
1-D1	2500-5000
2-D2	1250-2500
3-D3	625-1250
4-D4	312.5-625
5-D5	156.25-312.5
6-D6	78.125-156.25
7-D7	39.0625-78.0625
A7	19.5-39.025

The energy content in the details of each decomposition level for all voltage signals was calculated using the detail coefficients in the corresponding level. The energy content in the other decomposition levels can be estimated as:

$$\|ED_{1a}\| = \left[\sum_k d_k^2 \right]^{1/2} \quad (17)$$

Where ED_{1a} is the energy content of D1 for voltage signal of phase (a) and d_k is the k th coefficient in the first decomposition level. After collecting the characteristics for the simulated different cases, the characteristics will be fed to a trained ANN in order to identify whether the event took place is islanding or non-islanding event. The flow chart of the suggested procedure is demonstrated in Figure 8.

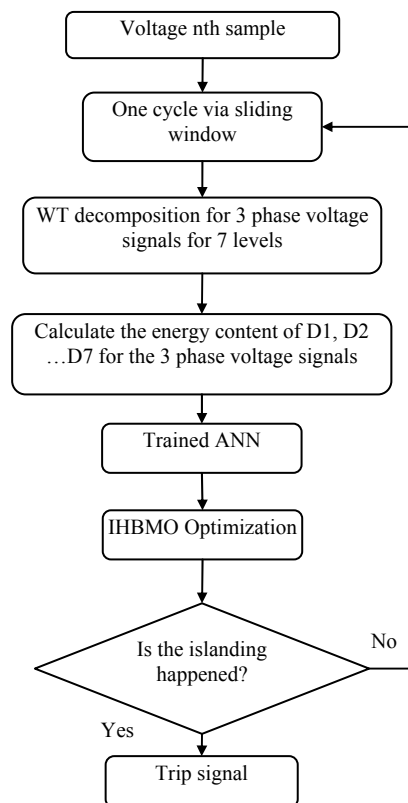


Figure 8. The flow chart of proposed technique for islanding detection

6. Simulation Results

In this part, the test system in Figure 9 has been simulated by MATLAB/Simulink. The system, DG, and load parameters are listed in [33]. The Effective voltage waveform of the common coupling point for islanding mode is shown in Figure 10.

Figure 11 to 13 show an example of the wavelet details (D3, D4 and D6) of 2 cycles voltage waveform acquired from phase (a) at DG when four different events have taken place. These events have taken place at time = 1.5 sec. In the suggested figures the islanding when power match (a), islanding when power mismatch (b), switching of load (c), and three-phase-to-ground fault (d), are shown. It is noticed from the graphs that during the fault the details dropped to zero since the DG is equipped with UOF/UOV protective relay which isolated the fault. Also, the Performance matrix of DG is demonstrated in Table 2.

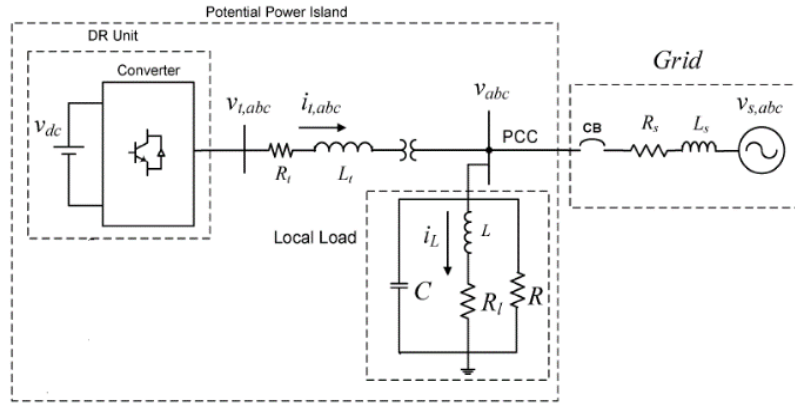


Figure 9. Schematic diagram of a grid-interfaced DG unit

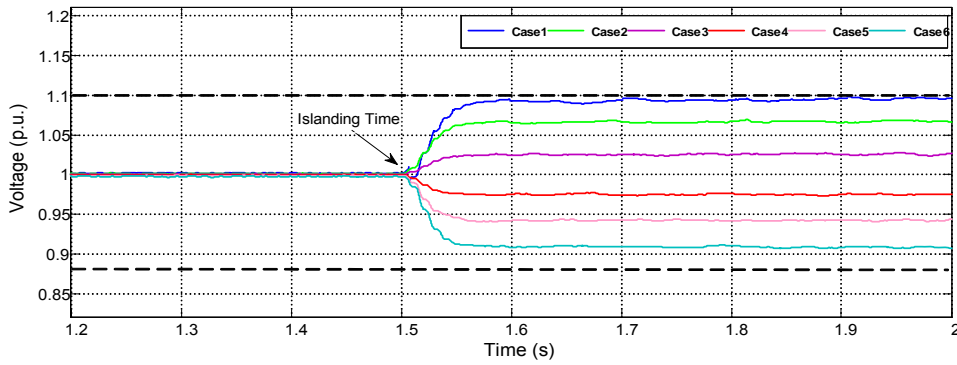


Figure 10. Effective voltage waveform of the common coupling point for islanding mode

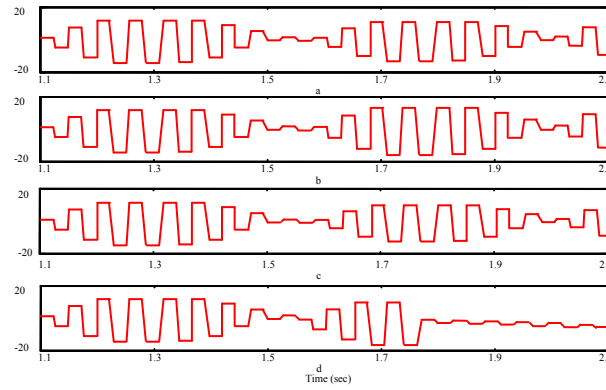


Figure 11. Wavelet detail D-3 of voltage waveform in case of (a) islanding when power match, (b) islanding when power mismatch, (c) switching of load, and (d) three-phase-to-ground fault.

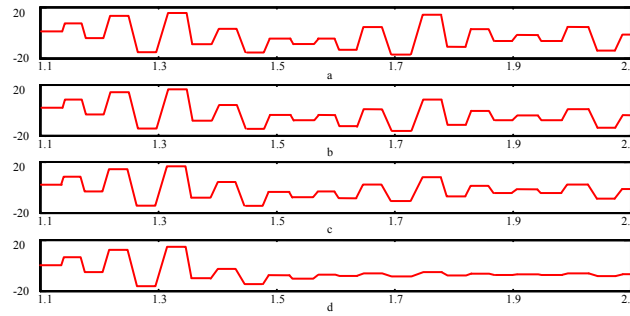


Figure 12. Wavelet detail D-4 of voltage waveform in case of (a) islanding when power match, (b) islanding when power mismatch, (c) switching of load, and (d) three-phase-to-ground fault.

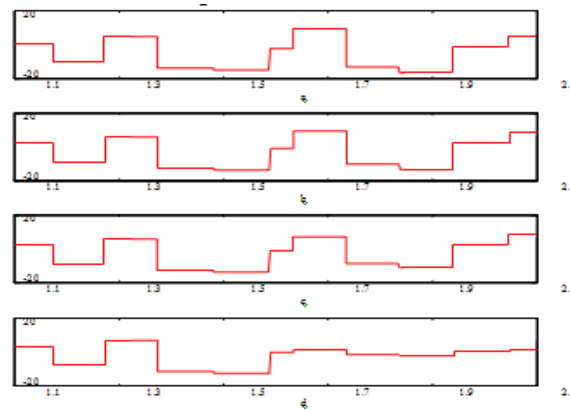


Figure 13. Wavelet detail D-6 of voltage waveform in case of (a) islanding when power match, (b) islanding when power mismatch, (c) switching of load, and (d) three-phase-to-ground fault.

Table 2. The Performance matrix of DG

		Islanding		Non-islanding		
		Matched	Switching of load	Switching of Capacitor bank	Faults	Normal operation
Islanding	Matched	20	0	0	0	0
Non-islanding	Switching of load	1	9	0	0	0
	Switching of Capacitor bank	0	0	10	0	0
	Faults	0	0	0	10	0
	Normal operation	0	0	0	0	10
Accuracy		98.70%				

6.1. Voltage deviation (Voltage Swell, Voltage Sag) in islanding detection method

Islanding detection procedure should be kept safe from voltage changes. By adding an adaptive system with a delay system, one can keep safe the detection procedure from the voltage changes. Therefore, the inverter output current is monitored continuously and once the difference between this current and threatened current is observed the comparator detects automatically these abnormal conditions. These abnormal conditions can be sign of either: a) an electrical island, b) voltage deviation. Table.3 shows Voltage relay responses when an abnormal condition is observed in the standard distribution network IEEESTd.1547. Simple voltage relays should detect the voltage changes at the appropriate time and then eliminates the distributed generation from the grid.

Table 3. Voltage relay responses

Voltage range (% of base voltage)	Clearing time (s)
V<50	0.16
50%<V<88	2
110<V<120	1
V>120%	0.16

Performance of the suggested procedure is analyzed in this mode for the various conditions which are given in the Table 4. Three phase voltage waveform of the common coupling point for each case are represented in Figure 14. Also rate of change of active power for all cases studied are shown in Figure 15. Immediately following these change at the time t = 1 sec, rate of change of active power for each condition are increased or decreased. Finally, in Fig.16 the output of detection method for all studied cases are shown. It is obvious from Figure 16 that after all studied cases value of the proposed algorithm has not changed and the output of proposed method is remained 0. Thus, the suggested procedure does not send a trip signal to distributed generation and works in a reliable mode.

Table 4. The various condition for voltage deviation test

	Case1	Case2	Case3	Case4	Case5	Case6
	One-Phase Fault	Two-Phase Fault	Two-Phase Fault	Three-Phase Fault	Three-Phase Fault	Three-Phase Fault
Fault Resistance (Ω)	1	0.1	1	0.05	0.1	1
Ground Resistance (Ω)	0.1	0.1	0.1	0.1	0.1	0.1

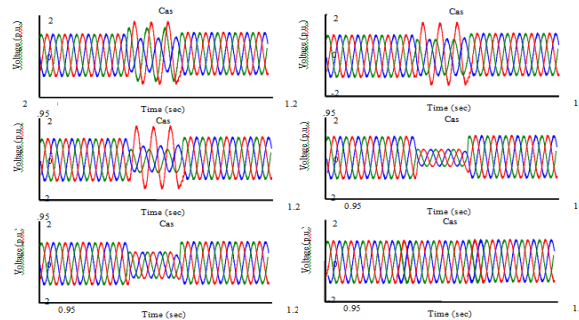


Figure 14. Three phase voltage waveform of the common coupling point for voltage deviation mode

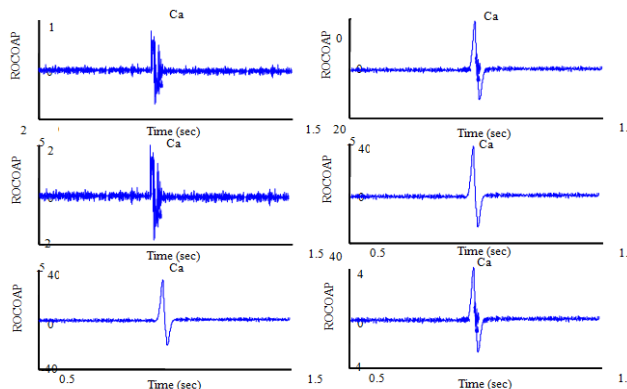


Figure 15. rate of change of active power for voltage deviation mode

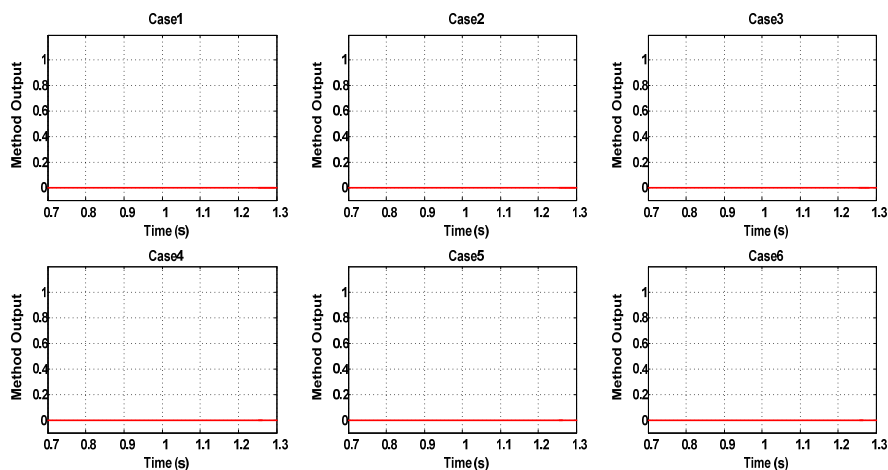


Figure 16. the output of detection method for voltage deviation mod

7. Conclusion

A new technique for islanding detection of distributed generation is suggested on the bases of Hybrid Wavelet Neural Network with Interactive Honey Bee Matting Optimization (IHBMO). Many schemes have been suggested to detect islanding such as passive, active and communication based procedures. Passive techniques work well when there is power imbalance between the power generated from the DG and the power consumed from the load. From the other point of view, active techniques affect the power quality and do not perform well in the presence of multiple DGs. The energy content of wavelet details are then calculated and fed to a trained ANN which is capable to differentiating between islanding and non-islanding events. Following the increased number and enlarged size of distributed generating units installed in a modern power system, the protection against islanding has become extremely challenging nowadays. The main emphasis of the proposed scheme is to decrease the NDZ to as close as possible and this procedure can also overcome the problem of setting the detection thresholds inherent in the existing techniques. Simulation results verified that the islanding cases were successfully detected in case of adding untrained identical DGs since the voltage transients generated is identical.

References

- [1] EF. El-Saadany, HH. Zeineldin, AH. Al-Badi. Distributed generation: benefits and challenges. International Conference on Communication, Computer & Power. 2007: 115-119.
- [2] A. Algarni. Operational and planning aspects of distribution systems in deregulated electricity markets. *Ph.D. dissertation*. University of Waterloo, Waterloo, ON, Canada. 2009.
- [3] HH. Zein El Din, EF. El-Saadany, MMA. Salama. Islanding Detection of Inverter Based Distributed Generation. in IEE Proceedings in Generation, Transmission and Distribution. 2006; 153(6): 644–652.
- [4] MA. Eltawil, Z. Zhao. Grid-connected photovoltaic power systems: Technical and potential problems—A review. *Renewable and Sustainable Energy Reviews*. 2009; 14: 112–129.
- [5] United States of America. *Congress of the U.S., Congressional Budget Office*. Prospects for distributed electricity generation. September. 2003.
- [6] Zeineldin HH, El-Saadany Ehab F, Salama MMA. Impact of DG interface control on islanding detection and non-detection zones. *IEEE Trans Power Delivery*. 2006; 21(3): 1515–23.
- [7] IEEE Standard for Interconnecting Distributed Resources into Electric Power Systems. IEEE Standard 1547TM. June 2003.
- [8] Hernandez-Gonzalez G, Iravani R. Current injection for active islanding detection of electronically-interfaced distributed resources. *IEEE Trans Power Delivery*. 2006; 21(3): 1698–705.
- [9] Karimi H, Yazdani A, Iravani R. Negative-sequence current injection for fast islanding detection of a distributed resource unit. *IEEE Trans Power Electr*. 2008; 23(1): 298–307.
- [10] Ropp ME, Begovic M, Rohatgi A. Analysis and performance assessment of the active frequency drift method of islanding prevention. *IEEE Trans Energy Convers*. 1999; 14(3): 810–6.

- [11] Hung GK, Chang CC, Chen CL. Automatic phase-shift method for islanding detection of grid-connected photovoltaic inverters. *IEEE Trans Energy Convers.* 2003; 18(1): 169–73.
- [12] Song kim. Islanding Detection Technique using Grid-Harmonic Parameters in the Photovoltaic System. *Energy Procedia.* 2012; 14: 137-141.
- [13] Wen-Jung Chiang, Hurng-LiahngJou, Jinn-Chang Wu, Kuen-Der Wu, Ya-Tsung Feng. Active islanding detection method for the grid-connected photovoltaic generation system. *Electric Power Systems Research.* 2010; 80(4): 372-379.
- [14] F. Hashemi, A. Kazemi, S. Soleymani. A New Algorithm to Detection of Anti-Islanding Based on dqo Transform. *Energy Procedia.* 2012; 14: 81-86.
- [15] Mohammad A. Choudhry, Hasham Khan. Power loss reduction in radial distribution system with multiple distributed energy resources through efficient islanding detection. *Energy.* 2010; 35(12): 4843-4861.
- [16] Jang S, Kim K. An islanding detection method for distributed generation algorithm using voltage unbalance and total harmonic distortion of current. *IEEE Trans Power Delivery.* 2004; 19(2): 745–52.
- [17] Lopes LAC, Zhang Y. Islanding detection assessment of multi-inverter systems with active frequency drifting methods. *IEEE Trans Power Delivery.* 2008; 23(1): 480–6.
- [18] ME. Ropp, M. Begovic, A. Rohatgi, GA. Kern, RH. Bonn, S. Gonzalez. Determining the relative effectiveness of islanding methods using phase criteria and nondetection zones. *IEEE Trans. Energy Conv.* 2000; 15(3): 290–296.
- [19] HH. Zeineldin, T. Abdel-Galil, EF. El-Saadany, MMA. Salama. Islanding detection of grid connected distributed generators using TLS-esprit. *Electric Power Syst. Res., Elsevier.* 2007; 77(2): 155–162.
- [20] SJ. Huang, FS. Pai. A new approach to islanding detection of dispersed generators with self-commutated static power converters. *IEEE Trans. Power Del.* 2000; 15(2): 500–507.
- [21] ST. Mak. A new method of generating TWACS type outbound signals for communication on power distribution networks. *IEEE Trans. Power App. Syst.* 1984; PAS-103(8): 2134–2140.
- [22] W. Xu, G. Zhang, C. Li, W. Wang, G. Wang, J. Kliber. A power line signaling based technique for anti-islanding protection of distributed generators—Part I: scheme and analysis a companion paper submitted for review.
- [23] Cheng-Tao Hsieh, Jeu-Min Lin, Shyh-Jier Huang. Enhancement of islanding-detection of distributed generation systems via wavelet transform-based approaches. *International Journal of Electrical Power & Energy Systems.* 2008; 30(10): 575-580.
- [24] Javidan J, Ghasemi A. Environmental/Economic Power Dispatch Using Multi-objective Honey Bee Mating Optimization. *International Review of Electrical Engineering (I.R.E.E.).* 2012; 7(1): 3667-75.
- [25] Niknam T, Mojarrad HD, Meymand HZ. A new honey bee mating optimization algorithm for non-smooth economic dispatch. *Energy.* 2011; 36: 896-908.
- [26] Niknam T. An efficient hybrid evolutionary algorithm based on PSO and HBMO algorithms for multi-objective Distribution Feeder Reconfiguration. *Energy Conversion and Management.* 2009; 50(8): 2074-82.
- [27] Ghasemi A, Shayanfar HA, Mohammad SN, Abedinia O. Optimal Placement and Tuning of Robust Multimachine PSS via HBMO. in Proceedings of the International Conference on Artificial Intelligence, Las Vegas, U.S.A. 2011: 201-8.
- [28] Z. Ye, A. Kolwalkar, Y. Zhang, P. Du, R. Walling. Evaluation of anti-islanding schemes based on nondetection zone concept. *IEEE Trans. Power Electron.* 2004; 19(5): 1171–1176.
- [29] C. Parameswariah, M. Cox. Frequency Characteristics of Wavelets. *IEEE Power Engineering Review.* 2002; 22.
- [30] Rocha Reis AJ, Alves da Silva AP. Feature Extraction via Multiresolution Analysis for Short-Term Load Forecasting. *IEEE Trans. on Power Systems.* 2005; 20: 189-198.
- [31] Conejo AJ, Plazas MA, Espinola R, Molina AB. Day-ahead electricity price forecasting using the wavelet transform and ARIMA models. *IEEE Trans. on Power Systems.* 2005; 20: 1035-1042.
- [32] S. Chen. Feature selection for identification and classification of power quality disturbances. *Power Engineering Society General Meeting.* 2005; 3: 2301-2306.
- [33] Farid Hashemi, Noradin Ghadimi, Behrooz Sobhani. Islanding detection for inverter-based DG coupled with using an adaptive neuro-fuzzy inference system. *Electrical Power and Energy Systems.* 2013; 45(1): 443–455.